JPET Fast Forward. Published on November 16, 2015 as DOI: 10.1124/jpet.115.228387
This article has not been copyedited and formatted. The final version may differ from this version.

JPET #228387

Title: Sigma-2 receptors play a role in cellular metabolism: Stimulation of glycolytic hallmarks by CM764 in human SK-N-SH neuroblastoma*

Hilary Nicholson, Christophe Mesangeau, Christopher R. McCurdy, and Wayne D. Bowen

Department of Molecular Pharmacology, Physiology, and Biotechnology, Brown University, Providence, RI (HN, WDB)

Department of BioMolecular Sciences, School of Pharmacy, University of Mississippi, University, MS (CM, CRM)

JPET #228387

Running title: Activation of sigma-2 receptor induces metabolic stimulation

Corresponding author:

Wayne D. Bowen, Ph.D.

171 Meeting Street

Box G-B389

Providence, RI 02912

401-863-3253 (p)

401-863-1595 (f)

Wayne_Bowen@brown.edu

Number of text pages: 26

Number of tables: 1

Number of figures: 12

Number of references: 41

Number of words in Abstract (250 max): 246

Number of words in Introduction (750 max): 750

Number of words in Discussion (1500 max): 1495

JPET Fast Forward. Published on November 16, 2015 as DOI: 10.1124/jpet.115.228387
This article has not been copyedited and formatted. The final version may differ from this version.

ABBREVIATIONS: BD1047, N'-[2-(3,4-dichlorophenyl)ethyl]-N,N,N'-trimethylethane-1,2-diamine; BD1063, 1-[2-(3,4-dichlorophenyl)ethyl]-4-methylpiperazine; CM572, 3-(4-(4-(4-fluorophenyl)piperazin-1-yl)butyl)-6-isothiocyanatobenzo[*d*]oxazol-2(3*H*)-one; CM764, 6-acetyl-3-(4-(4-(2-amino-4-fluorophenyl)piperazin-1-yl)butyl)benzo[d]oxazol-2(3H)-one; DCFDA, 2',7'-dichlorofluorescin diacetate; DFO, deferoxamine; DTG, 1,3-di-o-tolylguanidine; EDTA, ethylenediaminetetraacetic acid; HBSS, Hank's Balanced Salt Solution; HIF1α, hypoxia-inducible factor 1 alpha; MEM, Minimal Essential Media; MTT, 3-[4,5 dimethylthaizol-2-y]-2,5 diphenyltetrazolium bromide; NE100, 4-methoxy-3-(2-phenylethoxy)-N,N-dipropylbenzeneethanamine; PBS, phosphate buffered saline; PGRMC1, progesterone receptor membrane component 1; RIPA buffer, radioimmunoprecipitation assay buffer; ROS, reactive oxygen species; RT, room temperature; SN79, 6-acetyl-3-(4-(4-(4-fluorophenyl)piperazin-1-yl)butyl)benzo[d]oxazol-2(3H)-one; TBS, Tris buffered saline; VEGF, vascular endothelial growth factor.

Recommended section assignment: Cellular and Molecular

Abstract

Sigma-2 receptors are attractive anti-neoplastic targets due to their ability to induce apoptosis and their upregulation in rapidly proliferating cancer cells as compared to healthy tissue. However, this role is inconsistent with overexpression in cancer, which is typically associated with upregulation of pro-survival factors. Here we report a novel metabolic regulatory function for sigma-2 receptors.. CM764 (6-acetyl-3-(4-(4-(2-amino-4-fluorophenyl)piperazin-1-yl)butyl)benzo[d]oxazol-2(3H)-one) binds with Ki values of 86.6 ± 2.8 and 3.5 ± 0.9 nM at sigma-1 and sigma-2 receptors, respectively. CM764 increased reduction of MTT in human SK-N-SH neuroblastoma compared to untreated cells, an effect not due to proliferation. This effect was attenuated by five different sigma antagonists, including CM572, which has no significant affinity for sigma-1 receptors. This effect was also observed in MG-63 osteosarcoma and HEK293T cells, indicating that this function is not exclusive to neuroblastoma or to cancer cells. CM764 produced an immediate, robust, and transient increase in cytosolic calcium, consistent with sigma-2 receptor activation. Additionally, we observed an increase in total NAD^+/NADH level and ATP level in CM764-treated SK-N-SH cells as compared to untreated cells. After only 4 h treatment, basal levels of reactive oxygen species were reduced by 90% in cells treated with CM764 over untreated cells, and HIF1α and VEGF levels were increased after 3-24 h treatment. These data indicate that sigma-2 receptors may play a role in induction of glycolysis, representing a possible pro-survival function for the sigma-2 receptor that is consistent with its upregulation in cancer cells as compared to healthy tissue.

Introduction

The sigma receptors comprise a pharmacologically defined family of membrane bound receptors that bind compounds from a variety of structural classes. The sigma-1 receptor is a 25 kDa protein that demonstrates stereoselectivity for (+)-benzomorphans and is known to promote cell survival (Hayashi and Su 2003; Hayashi and Su 2007; Tsai et al. 2009). The sigma-2 receptor is a 21.5 kDa protein that binds (+)-benzomorphans poorly and is significantly upregulated in rapidly proliferating tumors as compared to noncancerous tissue (Hellewell and Bowen 1990; Vilner et al. 1995; Wheeler et al. 2000). The presence of sigma-2 receptors has been validated in an extensive list of human and rodent cancer cell lines and tumors, and thus a ubiquitous role in cancer biology has been proposed (Wheeler et al. 2000; Mach et al. 2013).

Upon activation, the sigma-2 receptor induces apoptotic cell death (Crawford and Bowen 2002; Zeng et al. 2012; Zeng et al. 2014). A variety of pathways have been described in response to sigma-2 receptor activation, indicating that there exists more than one mechanism of sigma-2 receptor-induced cell death (Zeng et al. 2012). Further, discrete ligands induce independent apoptotic pathways even within a cell type, again suggesting the ability of the sigma-2 receptor to activate multiple signaling pathways (Crawford and Bowen 2002; Cassano et al. 2009; Zeng et al. 2012; Cesen et al. 2013).

The sigma-2 receptor has received attention for its potential use as a chemotherapeutic target. The significant upregulation of sigma-2 receptors in cancer as compared to healthy tissue makes it a naturally cancer-selective target, and is currently being examined clinically for diagnostic tumor imaging (Mach et al. 2013; Shoghi et al. 2013). The induction of apoptosis upon activation combined with endogenous cancer cell selectivity makes the sigma-2 receptor an attractive target for chemotherapeutic intervention. We have recently shown that the irreversible

sigma-2 receptor partial agonist CM572 selectively induces cell death in neuroblastoma, pancreatic, and breast cancer cell lines compared to effects in normal epithelial melanocytes or normal breast epithelial cells (Nicholson et al. 2015). However, the wide variety of apoptotic mechanisms induced by sigma-2 receptor activation combined with a disparity among criteria for defining functional classes of sigma-2 receptor ligands make studying the efficacy of such drugs difficult.

One intrinsic question about sigma-2 receptors that has yet to be extensively addressed surrounds their endogenous function. The endogenous ligand for sigma-2 receptors has yet to be elucidated, thus all hypotheses surrounding sigma-2 receptor function are based on observations collected through manipulation with synthetic agents. The observed apoptotic response to treatment with sigma-2 receptor ligands is widely supported; however, it is inconsistent with upregulated expression in rapidly proliferating cancer cells. This counterintuitive role is further called into question when coupled with the low but significant expression of sigma-2 receptors in many non-cancerous tissues such as liver and kidney (Hellewell et al. 1994), which indicates a role for sigma-2 receptors outside of cancer cell proliferation.

Evidence for a non-apoptotic function of sigma-2 receptors is not yet extensive, however examples of such activity do exist. For example, one criterion for classification of a sigma-2 receptor agonist is stimulated transient release of calcium from thapsigargin-sensitive pools in the endoplasmic reticulum (Vilner and Bowen 2000; Cassano et al. 2009). However, this calcium signal is not a trigger for apoptosis, as cells appear normal if ligand is removed after the transient returns to baseline (unpublished observation). In addition, there are also sigma-2 ligands that produce a calcium signal, but do not have the ability to kill cells. The sigma-2 receptor ligand SN79 (Kaushal et al. 2011; Kaushal et al. 2012) produces a small calcium signal

in SK-N-SH neuroblastoma cells, but is unable to induce significant levels of cytotoxicity even at high doses (Garcia 2012). Based on such data we have proposed that the sigma-2 receptor may signal to pathways that bifurcate to those that result in apoptotic cell death and those that result in as yet uncharacterized non-apoptotic effects (Garcia et al. 2010; Garcia 2012).

Recently it was proposed that progesterone receptor membrane component-1 (PGRMC1) is the putative sigma-2 receptor binding site (Xu et al. 2011). In MCF-7 cells, PGRMC1 mediates a signal that stimulates proliferation and angiogenesis-related effects (Neubauer et al. 2009), further suggesting a non-apoptotic function for ligands binding PGRMC1 or the sigma-2 receptor, whether identical or pharmacologically related. Here, we report a novel non-apoptotic, metabolically stimulative function for the sigma-2 receptor, discovered through intervention with CM764, a novel derivative of SN79. This may suggest a divergent role of relevance to sigma-2 receptor upregulation.

Materials and Methods

Radioligand binding assay

Rat liver membrane homogenates were used for receptor binding assays with slight modification to the previously reported procedure (Hellewell et al. 1994). Frozen rat livers (BioChemed, Winchester, VA) were thawed and homogenized for membrane preparation as previously described (Hellewell et al. 1994). A 150 μg of membrane protein was incubated with 3 nM [^{3}H](+)-pentazocine (Perkin Elmer, Waltham, MA) (sigma-1 receptor condition) or 5 nM [^{3}H]DTG (Perkin Elmer, Waltham, MA) and 100 nM unlabeled (+)-pentazocine to mask sigma-1 receptors (sigma-2 receptor condition) with various concentrations of CM764 for 120 min at 25°C in 20 mM HEPES pH 7.4 with gentle shaking. Nonspecific binding was measured in the presence of 10 μM haloperidol. Membranes were collected by filtration using a Brandel Cell Harvester (Brandel, Gaithersburg, MD) onto glass fiber filters that were presoaked in 0.5% polyethyleneimine for 30 min at room temperature. Ice cold 10 mM Tris-HCl, pH 7.4 was used to terminate reactions using 5 mL buffer followed by two 5 mL buffer washes. Ki values were determined by competition binding assay and data analyzed using GraphPad Prism 6 (GraphPad Software, La Jolla, CA) with K_d=17.9 nM for [^{3}H]DTG at sigma-2 receptors and K_d=7.5 nM for [^{3}H](+)-pentazocine at sigma-1 receptors in rat liver membrane homogenates.

Cell culture

Human SK-N-SH neuroblastoma cells were obtained from ATCC (Manassas, VA) and were cultured in Minimal Essential Medium (Gibco, Grand Island, NY) with 10% fetal bovine serum and 10 mg/L human insulin (Gibco, Grand Island, NY) in a humidified atmosphere at 37°C and 5% CO_2. HEK 293 T/17 human embryonic kidney cells were a generous gift from Dr. Elena Oancea, Brown University, Providence, RI, and human MG-63 osteosarcoma cells were a generous gift from Dr. Eric Darling, Brown University, Providence, RI. Both additional cell types were cultured in the same way as described for SK-N-SH neuroblastoma. Cells were passaged at 70% confluency.

MTT cell viability assay

Cell viability was measured by MTT assay (Trevigen, Gaithersburg, MD). Cells were plated at 15,000 cells/well (SK-N-SH) or 10,000 cells/well (HEK 293 T/17, MG-63) in a 96-well plate and allowed to attach overnight. Cells were then treated for 24 h prior to addition of 10 µL MTT reagent, which was allowed to be metabolized into colored formazan crystals for 3 h. A 100 µL aliquot of MTT detergent reagent was then added and formazan crystals and cell membranes were solubilized for 2 h prior to reading absorbance at 570 nm. Data was analyzed in Microsoft Excel.

CyQUANT cell proliferation assay

Cellular proliferation was measured using the CyQUANT Cell Proliferation Assay Kit (Life Technologies, Grand Island, NY). Cells were plated in 96-well plates at 15,000 cells/well for 24-48 h experiments or 10,000 cells/well for 72-96 h experiments. Cells were allowed to attach overnight prior to treatment with 10 μM CM764 or fresh media without ligand (control). Media with or without ligand was replaced every 24 h. After the indicated time, cells were washed once with PBS and then plate was inverted and blotted dry onto a Kimwipe by gentle tapping, and frozen at -80ºC for at least 24 h. Plates were then thawed to RT and stained with 1X CyQUANT GR dye, which exhibits enhanced fluorescence when bound to nucleic acids, in cell lysis buffer for 5 min protected from light prior to measurement of fluorescence at 480nm excitation/520 nm emission.

Calcium Release Assay

Fura-2 was used to measure intracellular calcium in SK-N-SH neuroblastoma. Cells were seeded at 20,000 cells/well and allowed to attach overnight prior to washing twice with HBSS and loading for 60 minutes with 2.47 μM fura-2 acetoxymethyl ester (fura-2AM, Invitrogen, Grand Island, NY) in 0.065% pluronic acid in HBSS. Cells were then washed twice with HBSS prior to injection with indicated ligand. Stock solutions for injection were adjusted such that injection volume was 10 μL, injected onto 90 μL HBSS in the well for a final total volume of 100 μL. Fura-2 ratio was measured with excitation at 340 and 380 nm and emission at 510 nm using a PerkinElmer Victor V plate reader. A baseline ratio was determined prior to injection by

measuring 25 readings over 43 seconds, after which the 10 µL injection was made and 100 readings were measured.

NAD^+/NADH assay

NAD^+ and NADH were measured using the NAD^+/NADH Quantification Colorimetric Kit from BioVision (Milpitas, CA), which allows for determination of total NAD, NAD^+, and NADH from plated cells without the need for purification steps. Cells were plated in 35 mm petri dishes at 200,000 cells/dish and allowed to attach overnight prior to treatment with 10 µM CM764 or fresh media without ligand (control) for 24 h. NAD^+/NADH assay was then performed according to manufacturer's specifications. Cells were washed once with cold PBS, dissociated with 2.5 mM EDTA, pelleted by centrifugation at 223 x g for 5 min, and extracted with 400 µL Extraction Buffer by two freeze/thaw cycles of 20 min on dry ice and 10 min at room temperature. The extract was then pelleted by centrifugation at 37,500 x g for 5 min and supernatant was collected. For NADH determination, NAD^+ was degraded by 30 min heating at 60ºC. Samples were incubated with Reaction Mix for 5 min prior to the addition of 10 µL Developer, and then allowed to cycle for 4 h. Absorbance was measured every hour at 450 nm. NADt (NADH + NAD^+) and NADH levels were measured directly. NAD^+ level was inferred to be the difference between NADt and NADH. Protein concentration was measured by BCA assay (Pierce, Waltham, MA) and NADt/NADH/NAD^+ levels were adjusted for protein levels.

ATP assay

Cellular ATP was measured using an ATP Colorimetric/Fluorometric Assay Kit (BioVision, Milpitas, CA). Cells were plated in 35 mm petri dishes at 600,000 cells/well and allowed to attach overnight prior to treatment with 10 μM CM764 or fresh media without ligand (control). After 24 h, cells were washed once with PBS, lysed, and immediately deproteinized with perchloric acid and neutralized with potassium hydroxide. A 50 μL aliquot of deproteinized supernatant was incubated with Reaction Mix for 30 min at room temperature protected from light. Fluorescence of the samples was read at 535 nm excitation/587 nm emission. Protein concentration was measured by BCA assay (Pierce, Waltham, MA) and ATP levels were adjusted for protein levels.

Detection of cellular reactive oxygen species

Cells were plated in a black-sided 96-well plate at 25,000 cells/well and allowed to attach overnight. Cells were then washed once with HBSS and stained with 50 μM DCFDA (Abcam, Cambridge, MA) in HBSS for 45 min in the dark at 37ºC. Cells were washed once with HBSS and treated with indicated compound for 4 h in phenol red-free media with 200 μg/mL α-tocopherol as a negative control and 500 μM TBHP as a positive control. Fluorescence was measured at 485 nm excitation/535 nm emission.

Western blot

SK-N-SH neuroblastoma cells were plated in 35 mm petri dishes and allowed to attach overnight prior to treatment with 10 μM CM764 for indicated time. Cells were lysed in RIPA buffer containing Halt Protease and Phosphatase Inhibitor Cocktail (Thermo Scientific, Waltham, MA), and 200 μM deferoxamine. Standardization was performed after protein concentration analysis by BCA assay (Pierce, Waltham, MA). Samples were run in a 10% acrylamide gel and transferred at 50V for 2.5 h at 4ºC onto nitrocellulose paper prior to blocking for 1 h at RT in 10% milk/TBS/0.1% Tween-20. Blots were then washed three times with TBS/0.1% Tween-20 and probed with antibodies for HIF1α (1:100, Santa Cruz, Dallas, TX) or VEGF (1:100, Santa Cruz, Dallas, TX) with GAPDH (1:100, Santa Cruz, Dallas, TX) or β-tubulin (1:500, developed by Michael Klymkowsky at University of Colorado, Boulder, CO, obtained from the Developmental Studies Hybridoma Bank (NICHD of NIH), maintained at University of Iowa, Iowa City, Iowa) used as a loading control, in 10% milk/TBS/0.1% Tween-20 (or 5% BSA/TBS/0.1% Tween-20 for β-tubulin only) with overnight shaking at 4ºC. Blots continued to shake at RT for 1 h and were then washed three times with TBS/0.1% Tween-20 before 1 h RT incubation with 1:3000 rabbit secondary antibody (HIF1α probe, VEGF probe) (Santa Cruz, Dallas, TX) or 1:1000 mouse secondary antibody (GAPDH probe, β-tubulin probe) (Santa Cruz, Dallas, TX). Blots were then washed three times with TBS/0.1% Tween-20 and developed using SuperSignal West Pico Chemiluminescent Substrate (Pierce, Waltham, MA) per manufacturer's specifications. UltraCruz Autoradiography Film (Santa Cruz, Dallas, TX) was used to make film exposures, which were then analyzed using ImageJ software (NIH, Bethesda, MD). Protein levels were standardized using a loading control, then normalized to the level of the standardized untreated control.

Data Analysis

Data analysis was performed using Microsoft Excel and GraphPad Prism 6 (GraphPad Software, La Jolla, CA). For radioligand competition binding assays, Ki values were determined using GraphPad Prism 6 for nonlinear regression log(agonist) vs. normalized response with variable slope parameters.. For cell viability analysis, fura-2AM calcium assays, ATP assays, $NADH/NAD^+$ assays, and CyQUANT Cell Proliferation assays, data was analyzed using Microsoft Excel. Two-tailed t-tests were performed where appropriate using Microsoft Excel, and one-way ANOVAs were performed using GraphPad Prism 6. For one-way ANOVAs, Dunnet's post-hoc test was used where appropriate for comparison to control group. Power analysis was performed to 80% power using a power analysis calculator developed by the University of British Columbia Department of Statistics based on normal distributions.

Sigma receptor ligands

The ligands used in this study are shown in Table 1 along with their sigma receptor binding characteristics and reference citations. The synthesis of CM764 has been previously described (McCurdy et al., 2014).

Results

Radioligand binding competition of CM764 at sigma-1 and sigma-2 receptors

The novel SN79 derivative CM764 is derived by the addition of an amine group to the fluorophenyl ring of SN79 (synthesis previously described) (McCurdy et al. 2014). The structures of both ligands are shown in Figure 1. Competition binding was performed using [^{3}H](+)-pentazocine to measure sigma-1 receptor binding and [^{3}H]DTG in the presence of unlabeled (+)-pentazocine to measure sigma-2 receptor binding as described in Methods. Complete radioligand competition curves are shown in Figure 2. CM764 binds sigma-2 receptors with ~25-fold selectivity over sigma-1 receptors, with Ki values of 3.5 ± 0.9 nM at sigma-2 receptors and 86.6 ± 2.8 nM at sigma-1 receptors. This is an increase in selectivity of 5-fold over the parent compound, SN79 (Ki=7 nM and 27 nM at sigma-2 and sigma-1, respectively) (Kaushal et al. 2011).

CM764-induced MTT reduction in SK-N-SH neuroblastoma

A well-established indicator of sigma-2 receptor activation is cell death. As CM764 was found to bind sigma-2 receptors well, we examined the effect of CM764 treatment on cell viability in order to determine the agonist or antagonist properties of the ligand. A commonly used assay to measure effects of agents on cell viability or proliferation is the MTT assay. The assay is based on the premise that reduction of the tetrazolium dye MTT to the colored formazan product, mainly in mitochondria and cytosol, is proportional to the number of viable cells. Thus,

a decrease in MTT reduction usually indicates fewer cells and a cytotoxic effect, and this is the effect produced by sigma-2 receptor agonists. Human SK-N-SH neuroblastoma cells highly express sigma-2 receptors and have been demonstrated to be highly sensitive to sigma-2 receptor modulators, and were thus used to determine effects of CM764 on MTT reduction. (Vilner et al. 1995; Vilner and Bowen 2000; Hazelwood and Bowen 2006). The results are shown in Figure 3. Interestingly, treatment of SK-N-SH neuroblastoma cells with CM764 induced a dose-dependent *increase* in MTT reduction as compared to untreated control cells. This increase in MTT reduction was found to be statistically significant at 3 and 10 μM doses.

Effect of CM764 treatment on proliferation in SK-N-SH neuroblastoma

The increase in MTT reduction that resulted from treatment of SK-N-SH neuroblastoma with CM764 could occur from two potential causes: 1) an increased number of cells available to reduce MTT as compared to the untreated control condition, and/or 2) some direct effect to increase the activity of the enzymes that reduce MTT in each treated cell as compared to untreated cells. In order to determine whether the CM764-induced increase in MTT reduction was a result of increased cellular proliferation and therefore more cells being available to reduce MTT, the CyQUANT Cell Proliferation Assay was used to measure DNA replication. Cells were treated with CM764 for up to four days prior to staining with CyQUANT GR dye and quantification as described in Methods. Results are shown in Figure 4. There was no significant difference in DNA replication observed at any time point up to four days between cells treated with 10 μM CM764 and untreated control cells. In addition, these results were confirmed by counting DAPI-stained cells, which showed no significant differences between treated and

control groups (data not shown). These data indicate that treatment of SK-N-SH neuroblastoma cells with 10 μM CM764 does not result in increased DNA replication or cellular proliferation above that of normal cell turnover and proliferation. The results further show that treatment for longer than 24 h, up to 4 days, had no toxic effect on the cells. Thus, the increased reduction of MTT observed in CM764-treated cells could be attributed to stimulated reductive metabolism without a concurrent stimulation of cell division.

Pharmacological characterization of CM764-induced MTT reduction

The stimulative effect demonstrated by CM764 treatment of SK-N-SH neuroblastoma cells has yet to be reported as a result of sigma-2 receptor activation, which has previously only been associated with a decrease in cell viability (agonist activity). In order to determine whether the stimulation of MTT reduction induced by CM764 treatment is mediated by the sigma-2 receptor, several sigma-2 receptor modulators were investigated in combination with CM764 treatment to determine if the effect could be attenuated. The effects of known sigma receptor antagonists are shown in Figure 5. CM764 and each antagonist were dosed simultaneously and MTT reduction was measured after 24 h treatment. All sigma-2 receptor antagonists examined were able to significantly attenuate the stimulation of MTT reduction induced by CM764 alone, without inducing significant effect on MTT reduction when used alone. The well-characterized sigma-2 receptor antagonist SN79, the parent compound for CM764, was able to completely eliminate the stimulation induced by CM764 alone. A 24 h treatment of 30 μM SN79 alone had no significant effect on MTT reduction in SK-N-SH neuroblastoma as compared to an untreated control. Similarly, 0.3 μM CM572 a sigma-2 receptor partial agonist (Ki=15 nM at sigma-2

JPET Fast Forward. Published on November 16, 2015 as DOI: 10.1124/jpet.115.228387
This article has not been copyedited and formatted. The final version may differ from this version.

receptors and ≥10 μM at sigma-1 receptors), which we have previously shown has antagonist properties at this concentration in SK-N-SH neuroblastoma (Nicholson et al., 2015), eliminated CM764-induced MTT hyper-reduction when dosed in combination with 10 μM CM764. Sigma-1/sigma-2 antagonists BD1047 (Ki=47 nM at sigma-2 receptors and 0.93 nM at sigma-1 receptors (Matsumoto et al. 1995)) and BD1063 (Ki=449 nM at sigma-2 receptors and 9.15 nM at sigma-1 receptors (Matsumoto et al. 1995)) were both able to eliminate the increase in MTT reduction induced by CM764 treatment alone. NE100, which has selectivity for the sigma-1 receptor yet still has measurable affinity for the sigma-2 receptor (Ki=84.7 nM at sigma-2 receptors and 1.54 nM at sigma-1 receptors (Chaki et al. 1994)) was able to significantly attenuate but not completely eliminate the signal produced by CM764 when it was dosed in combination at 1 μM. The ability of these sigma-2 receptor modulators to attenuate or entirely eliminate the CM764-induced increase in MTT reduction in SK-N-SH neuroblastoma indicate that this effect is sigma-2 mediated and represents a novel function for this receptor.

CM764 does exhibit significant affinity for the sigma-1 receptor, although it is a sigma-2-selective ligand. Some of the ligands investigated for antagonist activity against CM764 are selective for the sigma-1 receptor, though doses used in these experiments were all at least 200-fold greater than the sigma-2 receptor Ki of the ligands and therefore could be expected to be acting at the sigma-2 receptor as well as the sigma-1 receptor. In light of this, it was necessary to examine whether the stimulation of MTT reduction observed in SK-N-SH neuroblastoma in response to treatment with CM764 could be a result of sigma-1 receptor activation either exclusively or in addition to sigma-2 receptor activation. To test this, the effect of treatment with the sigma-1 agonist (+)-pentazocine (K_i=1,542 nM at sigma-2 receptors and K_d =7.5 nM at sigma-1 receptors (Hellewell et al. 1994)) was examined in SK-N-SH cells. (+)-Pentazocine was

unable to induce any significant change in MTT reduction as compared to untreated control cells up to 1 μM, which is over 130-fold above its sigma-1 receptor Ki value (experiment was repeated twice with similar results, with 5 replicates per condition in each experiment). Additionally, CM572 was able to completely attenuate the effect of CM764 on MTT reduction, although CM572 exhibits no significant binding at the sigma-1 receptor. This antagonism demonstrates that the stimulation of MTT reduction induced by CM764 treatment could be entirely eliminated by selectively blocking the sigma-2 receptor, without blocking the sigma-1 receptor at all. These data confirm that this effect is sigma-2 receptor-mediated and does not involve sigma-1 receptors.

Effect of CM764 treatment on intracellular calcium

A common characteristic of sigma-2 receptor activation is an immediate, transient increase in intracellular calcium. However, this calcium response has not been consistently coupled to apoptosis. We therefore examined whether CM764 would induce this nontoxic calcium transient, commonly resultant from sigma-2 receptor activation. Using fura-2AM ratiometric dye, we determined that injection of CM764 for a final concentration of 10 μM and 30 μM both induced a robust, immediate calcium transient, with calcium level decreasing towards baseline within the 5-minute recording. The higher dose of CM764 reached a slightly greater peak increase in calcium level, and within a faster timeframe than the lower dose. This data indicates that CM764 is able to induce the immediate calcium transient characteristic of sigma-2 receptor activation, and confirms that this signal can occur independently from the induction of apoptosis.

Effect of CM764 on NAD^+/NADH levels

Since MTT dye is reduced to formazan by cellular reductase enzymes that are mainly found in mitochondria and cytosol (although also present in lysosomes and endosomes) (Liu et al., 1997), these data suggest that CM764 treatment stimulates these enzymes to increase their activity. Several oxidoreductase enzymes responsible for the reduction of MTT into formazan are known to be NADH-dependent (Berridge et al., 2005). We therefore tested whether the increase in MTT reduction exhibited in SK-N-SH cells upon treatment with CM764 could be reflected in an increase in levels of this cofactor, which could facilitate enzyme activity. Using a colorimetric kit for quantification of NAD^+/NADH levels, we were able to determine that there was a statistically significant increase in total NAD (sum of NADH and NAD^+) in cells treated with 10 μM CM764 for 24 h as compared with untreated cells. Results are shown in Figure 7. For both NAD^+ individually and NADH individually neither measurement reached a statistically significant change from untreated cells. This appears to be due to variability between which reduction state increased more than the other, as NAD^+ levels were determined indirectly as the difference between NAD total and NADH, which were both measured directly. Therefore, the variability in NAD^+ levels was dependent on the variability in NADH measurements, which did not allow for significance in NAD^+ unless significance was reached for NADH. However, the overall increase in total NAD in CM764-treated cells as compared to untreated cells demonstrate that increased levels of the cofactor required for enzymatic reduction of MTT was indeed induced by CM764. This is likely a contributing factor to the observed increase in MTT reduction in CM764-treated cells, perhaps in addition to direct stimulation of oxidoreductase enzymes.

Effect of CM764 treatment on ATP level

The increase in NADt and reduction of MTT that were induced by CM764 treatment of SK-N-SH neuroblastoma cells indicate an overall increase in metabolic function. In order to test this hypothesis, we measured ATP levels in CM764-treated cells as compared to untreated cells using a fluorescent kit as described in Methods. Results are shown in Figure 8. Cells treated for 24 h with 10 μM CM764 showed a modest yet statistically significant increase in ATP with average ATP levels being 13% higher in treated cells as compared to untreated cells (range of 8% to 23%). These data suggest that CM764 treatment does indeed stimulate metabolism, perhaps through induction of glycolysis rather than TCA cycle. TCA cycle stimulation would be expected to create a more significant increase in ATP as compared to the addition of glycolysis, which would produce only a modest increase in ATP production.

CM764-induced production of reactive oxygen species

Under glycolysis cells produce pyruvate, which can act as an antioxidant. Further, if some ATP production that results from oxidative phosphorylation in untreated cells were indeed resulting from glycolysis in CM764-treated cells as hypothesized above, then we would expect to see a decrease in reactive oxygen species generated from oxygen consumption in oxidative phosphorylation. In order to determine whether this effect could result from CM764 treatment, we measured ROS accumulation using the ROS-sensitive DCFDA dye. Cells were stained with DCFDA and then treated with 10 μM CM764 for 4 h prior to measurement of fluorescence as described in Methods. Results are shown in Figure 9. To ensure effectiveness of the assay, *tert*-

butyl hydrogen peroxide (TBHP) was used as a positive control (Panel A) as compared to untreated DCFDA-stained cells, which were normalized to 100% RFU. Basal fluorescence of unstained cells was subtracted from each measurement. As a negative control, treatment of SK-N-SH neuroblastoma with the antioxidant α-tocopherol (Vitamin E) showed a decrease in ROS of 76% as compared to an untreated control. Treatment with 10 μM CM764 for just 4 h showed a decrease in ROS of 95% as compared to an untreated control. These data indicate a very significant decrease in ROS in response to treatment with CM764, indicating a strong antioxidant effect resultant from activation of the sigma-2 receptor through this mechanism. This may be due to induction of glycolysis, which could explain the antioxidant effect of CM764 treatment.

In order to determine whether the reduction in ROS induced by treatment with CM764 was a result of direct radical scavenging, as with α-tocopherol, the experiment was repeated using 10 μM CM572. CM572 is a close structural analog of CM764, lacking the amine group on the fluorophenyl ring and instead having an isothiocyanate moiety on the heterocyclic ring system. A 10 μM dose of CM572 did not induce an increase in MTT reduction as compared to control cells, and also did not result in any significant change in level of ROS as compared to untreated cells even after 6 h of treatment (experiment was performed using 4 replicates per condition; data not shown). Thus the effect of CM764 on ROS is due to a signaling mechanism and not to direct radical scavenging.

Effect of CM764 on HIF1α protein level

A hallmark of cells undergoing glycolysis under normoxic conditions (aerobic glycolysis) is the expression of HIF1α. A link between treatment of tumor cells with the sigma modulator

JPET Fast Forward. Published on November 16, 2015 as DOI: 10.1124/jpet.115.228387
This article has not been copyedited and formatted. The final version may differ from this version.

rimcazole and increased expression of HIF1α has been established previously (Achison et al. 2007). We therefore decided to investigate whether this transiently expressed protein might be stabilized or increasingly translated upon treatment with CM764. Cell lysates of SK-N-SH neuroblastoma were made after treatment with 10 μM CM764 for the indicated length of time and were used to Western blot for presence of HIF1α as described in Methods. A representative blot of HIF1α and loading control GADPH are shown (Panel A) and quantified (Panel B) in Figure 10. Our results indicate a strong induction of HIF1α, either by stabilization of the translated protein or by increased translation of mRNA, in response to treatment with CM764. Increased expression was most significant after 24 h, showing >14-fold induction, however expression was already >4-fold increased after only 6 h treatment. The observed induction of HIF1α protein level is consistent with previous data that shows increased expression of HIF1α in cells that preferentially employ glycolysis under conditions of normoxia (Dery et al., 2005; Kuschel et al., 2012). These data suggest that CM764 treatment does induce aerobic glycolysis in SK-N-SH neuroblastoma cells, consistent with our results from ROS and ATP studies described above.

Effect of CM764 on VEGF protein level

To confirm the activity of increased HIF1α protein levels in SK-N-SH neuroblastoma cells in response to treatment with 10 μM CM764, a transcriptional target of HIF1α was measured in response to the same treatment. Vascular endothelial growth factor (VEGF) has been extensively described as a target of HIF1α transcriptional regulation, and anti-VEGF therapy has been shown to impair ATP level (Curtarello et al., 2015). We therefore examined the

effect of CM764 treatment on VEGF expression in SK-N-SH neuroblastoma. Results are shown (Panel A) and quantified (Panel B) in Figure 11. Our results confirm that protein level of VEGF is increased by over 4-fold in cells treated with 10 μM CM764 as compared to untreated cells. This increased expression was most significant after 24 h treatment, lagging behind the observed increased expression of HIF1α, which presumably regulated the VEGF transcription.

Effect of CM764 across multiple cell types

In order to determine whether the increase in MTT reduction induced by CM764 treatment is exclusive to SK-N-SH neuroblastoma, the effect of this treatment was investigated in multiple cell lines. Human embryonic kidney (HEK293 T/17) cells and human osteosarcoma (MG-63) cells were treated with CM764 at the indicated doses for 24 h prior to MTT assay. Results are shown in Figure 12. Maximal stimulation achieved with 10 μM CM764 in SK-N-SH neuroblastoma after 24 h treatment was matched using the same treatment in HEK293 T/17 cells and MG-63 cells. These data demonstrate that the increased reduction of MTT induced by CM764 activity at sigma-2 receptors is not exclusive to one cell type but rather may be present across a variety of cell types. Additionally, this effect is not exclusive to cancerous cell lines, as it is also effective in non-cancerous HEK cells, though there may be a slight trend toward less activity in the HEK cells compared to SK-N-SH and MG-63 cells at the lower concentrations. Together, these data suggest a role for sigma-2 receptors outside of cytotoxicity in cancer cells.

Discussion

Here we demonstrate a previously unreported metabolic regulatory role of sigma-2 receptors. CM764 binds sigma-2 receptors with high affinity (Ki=3.5 nM) and 25-fold selectivity over sigma-1 receptors (Figure 2), a significant increase in selectivity over the parent compound SN79. Since sigma-2 receptor activation has traditionally been associated with a reduction in cell viability, we used the MTT assay to measure potential loss of cell viability in response to CM764 exposure. Interestingly, treatment of SK-N-SH neuroblastoma cells with CM764 resulted in a significant increase in MTT reduction compared to untreated cells (Figure 3). This could result from cellular proliferation, stimulation of oxidoreductase activity, or both. Results from CyQUANT cell proliferation assays indicated no change in proliferation or DNA replication in response to treatment with CM764, suggesting a strictly metabolic effect (Figure 4).

This stimulative effect on MTT reduction could be attenuated by sigma-2 receptor antagonists with and without measurable affinity at sigma-1 receptors, but could not be replicated by sigma-1 receptor activation by sigma-1-selective agonist (+)-pentazocine. All sigma-2 receptor modulators investigated attenuated CM764-induced stimulation of MTT reduction while no effect on MTT reduction was observed for each antagonist independently (Figure 5). Specifically of note is the attenuation of the CM764-induced increase in MTT reduction by antagonism with CM572, which has high affinity for the sigma-2 receptor (Ki=15 nM) but no significant affinity for the sigma-1 receptor (Ki≥10,000 nM). These data indicate that this is a novel sigma-2-mediated effect that is independent of sigma-1 receptor activation.

JPET Fast Forward. Published on November 16, 2015 as DOI: 10.1124/jpet.115.228387
This article has not been copyedited and formatted. The final version may differ from this version.

CM764 injection onto fura-2-loaded SK-N-SH neuroblastoma cells induced an immediate, robust, transient calcium response, consistent with previous reports of sigma-2 receptor activation (Figure 6). This observation lends further support to the action of CM764 at sigma-2 receptors, as well as confirms that this calcium response can be uncoupled from induction of apoptosis. As changes in calcium level are also known to be early steps in several important metabolic pathways, this data is also consistent with a metabolic effect resultant from sigma-2 receptor activation by CM764.

As reduction of MTT is known to be NADH-dependent, NADH/NAD^+ levels were investigated in response to CM764 treatment. CM764 treatment induced an increase in total NAD (NADH + NAD^+) compared to untreated cells, indicating that levels of this cofactor are increased as a result of sigma-2 receptor activation by CM764 (Figure 7). However, the increase was modest, and while likely not limiting, the increase in NADH induced by CM764 activation of sigma-2 receptors is unlikely to be the driving factor for the observed increase in MTT reduction. The increase in NADt observed in response to CM764 treatment indicated moderate stimulation of a metabolic pathway, perhaps less efficient than an overall stimulation of oxidative phosphorylation.

CM764 also induced an increase in ATP levels of treated cells compared to untreated cells, further indicating a metabolic stimulation (Figure 8). However, this increase was modest (~13% increase in ATP level as compared to untreated control). CM764 also induced extensive reduction of ROS in SK-N-SH neuroblastoma as compared to untreated cells (Figure 9B). This effect was rapid, with near-complete elimination of basal levels of ROS occurring within 4 h of treatment. Interestingly, Ostenfeld et al. showed that the sigma-2 agonist siramesine caused an *increase* in ROS in WEHI-S fibrosarcoma and MCF-7 breast tumor cells that contributed to cell

death (Ostenfeld et al., 2005). In addition, methamphetamine may induce ROS production and cell death in differentiated NG108-15 neuroblastoma-glioma hybrid cells via activation of sigma-2 receptors that is antagonized by SN79 (Kaushal et al., 2014). These opposing effects on ROS by sigma-2 ligands are consistent with the notion of bifurcating toxic and non-toxic pathways mediated by sigma-2 receptors.

The modest increase in ATP levels and NADH could possibly be explained by the hypothesis that CM764 induces stimulation of glycolysis, rather than oxidative phosphorylation. Stimulation of glycolysis would add only a small amount of both of these factors in comparison to the highly efficient production of ATP and increased reduction of NAD^+ occurring by oxidative phosphorylation. The reduction in ROS observed in response to treatment with CM764 is also consistent with a hypothesis that CM764 induces stimulation of glycolysis, as the glycolytic pathway can reduce ROS in two ways. First, a product of glycolysis is pyruvate, which has antioxidant properties. Second, preferential use of glycolysis for ATP production can reduce oxidative phosphorylation, which decreases the amount of oxygen channeled into superoxide formation. Thus induction of glycolysis by CM764 is consistent with the observed ATP, $NADH/NAD^+$, and ROS data.

CM764 induced an increase in HIF1α protein level, known to be stabilized under conditions of aerobic glycolysis (Figure 10). Induction of HIF1α by CM764 treatment is consistent with activation of glycolysis, and has been shown to be induced without hypoxia in such cases. Further, CM764 treatment also induced expression of VEGF, a transcriptional target of HIF1α (Figure 11). This suggests that the HIF1α protein level increase is active protein, as the increased expression in VEGF followed ~18 h after the first significant observed increase in HIF1α, which occurred after 6 h of treatment. Taken together, these data suggest that CM764

induces a sigma-2-modulated stimulation of cellular glycolysis under normoxia. This is a novel function of the sigma-2 receptor that is more consistent with observations of sigma-2 receptor expression in rapidly proliferating non-cancerous cells such as HEK (Johannessen et al. 2009; Xu et al. 2011) and COS (Monassier et al. 2007; Johannessen et al. 2009) cells, as well as in tumor cells, as it may offer protection against damage from reactive oxygen species. Consistent with this hypothesis, CM764 induced an increase in MTT reduction that matched that induced in SK-N-SH neuroblastoma cells when dosed in human embryonic kidney cells and human osteosarcoma cells indicating that this effect is present across a variety of tumor and noncancerous cell types.

Overexpression of HIF1α is a common observation in many cancers (Zhong et al. 1999; Talks et al. 2000). HIF1α allows cells to overcome hypoxic conditions, as are common in the core of tumors and for metastases that may not have an established blood supply. Further, through its transcriptional activation of VEGF, HIF1α promotes angiogenesis and therefore oxygen supply for metastatic sites (Lin et al. 2004; Liang et al. 2008; Kim et al. 2014). The novel function of the sigma-2 receptor that our study has revealed is consistent with this role of HIF1α in rapidly proliferating cancer cells and allows for congruous explanation of the high expression of sigma-2 receptors in the same. Interestingly, sigma-1 receptors have also been linked to HIF1α. Blockade of sigma-1 receptors by the putative antagonist rimcazole in normoxic colorectal and mammary carcinoma cells increases HIF1α, but with a cytotoxic effect in this case (Achison et al., 2007). Thus, regulation of HIF1α by sigma-1 and sigma-2 receptor subtypes may be complex, with different viability outcomes depending on cell type and sigma ligand.

It has been proposed that the sigma-2 receptor binding site resides within the PGRMC1 protein complex (Xu et al. 2011). However, whether the sigma-2 receptor and PGRMC1 are one

in the same molecule remains controversial (Abate et al., 2015; Chu et al., 2015). Furthermore, the physiological effects of PGRMC1 activation have largely been shown to promote cell survival and inhibit apoptosis, which is in direct contrast with classical pro-apoptotic models of sigma-2 receptor activation (Losel et al. 2008; Neubauer et al. 2009; Ahmed et al. 2010; Peluso et al. 2010). Interestingly, activation of PGRMC1 by cell-impermeable progesterone was shown to significantly stimulate VEGF gene expression in MCF-7 cells (Neubauer et al., 2009). The data shown in Figure 5 and the lack of (+)-pentazocine activity show that the pharmacological profile of CM764-induced stimulation of MTT reduction is consistent with mediation by sigma-2 receptors. Yet stimulation of VEGF expression by CM764 resembles an effect of PGMRC1 activation (Neubauer et al., 2009). In view of the controversy over the identity of the sigma-2 receptor, there are three possible explanations for the data reported here: 1) the sigma-2 receptor is the binding site of PGRMC1, with bifurcating apoptotic and non-apoptotic pathways being initiated from a single sigma-2/PGRMC1 receptor entity, depending on the specific ligand involved, 2) PGRMC1 and sigma-2 receptors are distinct molecules, but have overlapping pharmacological profiles allowing some sigma-2 ligands to have effects at PGRMC1, or 3) PGRMC1 and sigma-2 receptors are distinct entitites with distinct pharmacological profiles, but binding of some compounds to sigma-2 receptors results in complexation with PGRMC1 and activation of non-toxic PGRMC1 signaling events. Distinguishing these possibilities will require further investigation. It should be mentioned here that several other SN79 analogs with high sigma-2 affinity are also able to stimulate MTT reduction (in preparation). In deference to the observed pharmacological profile, we have referred to the effects described herein as being sigma-2 receptor-mediated.

In conclusion, this study unveils a novel metabolically stimulative, non-toxic sigma-2 receptor function. It is consistent with an evolutionary benefit to upregulation of sigma-2 receptors in cancer cells and rapidly proliferating noncancerous cells, suggesting potential for protection against oxidative damage, hypoxic conditions, and stimulation of angiogenesis via VEGF production.

Acknowledgments

We thank Dr. Elena Oancea (Brown University) for her generous gift of HEK 293 T/17 cells.

We thank Dr. Eric Darling (Brown University) for his generous gift of MG-63 osteosarcoma cells.

Authorship contributions

Participated in research design: Nicholson, Bowen

Conducted experiments: Nicholson

Contributed new reagents or analytic tools: Mesangeau, McCurdy

Performed data analysis: Nicholson

Wrote or contributed to the writing of the manuscript: Nicholson, Bowen

References

Abate C, Niso M, Infantino V, Menga A, and Berardi F (2015) Elements in support of the 'non-identity' of the PGRMC1 protein with the sigma(2) receptor. *Eur J Pharmacol* **758**: 16-23.

Achison M, Boylan MT, Hupp TR, and Spruce BA (2007) HIF-1alpha contributes to tumour-selective killing by the sigma receptor antagonist rimcazole. *Oncogene* **26**(8): 1137-1146.

Ahmed IS, Rohe HJ, Twist KE, Mattingly MN, and Craven RJ (2010) Progesterone Receptor Membrane Component 1 (Pgrmc1): A heme-1 domain protein that promotes tumorigenesis and is Inhibited by a small molecule. *J Pharmacol Exp Ther* **333**(2): 564-573.

Cassano G, Gasparre G, Niso M, Contino M, Scalera V, and Colabufo NA (2009). F281, synthetic agonist of the sigma-2 receptor, induces Ca^{2+} efflux from the endoplasmic reticulum and mitochondria in SK-N-SH cells. *Cell Calcium* **45**(4): 340-345.

Cesen MH, Repnik U, Turk V, and Turk B (2013). Siramesine triggers cell death through destabilisation of mitochondria, but not lysosomes. *Cell Death & Disease* **4**.

Chaki S, Tanaka M, Muramatsu M, and Otomo S (1994). NE-100, a novel potent sigma-ligand, preferentially binds to sigma(1) binding-sites in guinea-pig brain. *Eur J Pharmacol* **251**(1): R1-R2.

Chu U, Mavlyutov T, Chu ML, Yang H, Mesangeau C, McCurdy C, Guo LW, and Ruoho A (2015) The 18 kDa sigma-2 receptor and PGRMC1 are derived from separate genes. *FASEB J* **29**(1).

Crawford K W and Bowen WD (2002) Sigma-2 receptor agonists activate a novel apoptotic pathway and potentiate antineoplastic drugs in breast tumor cell lines. *Cancer Res* **62**(1): 313-322.

Garcia D and Bowen WD (2010) Sigma-2 receptor-mediated apoptosis and calcium signaling: Are they bifurcating pathways? Society for Neuroscience, San Diego, CA, Meeting Planner. Program No. 470.17.

Garcia DR (2012) Sigma-2 receptor-mediated cytotoxicity and calcium signaling: Evidence for bifurcating pathways. PhD thesis, Brown University.

Hayashi T and Su T-P (2003) Intracellular dynamics of sigma-1 receptors (sigma(1) binding sites) in NG108-15 cells. *J Pharmacol Exp Ther* **306**(2): 726-733.

Hayashi T and Su T-P (2007) Sigma-1 receptor chaperones at the ER-Mitochondrion interface regulate Ca2+ signaling and cell survival. *Cell* **131**(3): 596-610.

Hazelwood S and Bowen WD (2006) Sigma-2 receptor-mediated apoptosis in human SK-N-SH neuroblastoma cells: Role of lipid rafts, caspases, and mitochondrial depolarization. *Proceedings of the American Association for Cancer Research* **47**: #4932.

Hellewell SB and Bowen WD (1990) A sigma-like binding site in rat pheochromocytoma (PC12) cells: decreased affinity for (+)-benzomorphans and lower molecular weight suggest a different sigma receptor form from that of guinea pig brain. *Brain Res* **527**(2): 244-253.

Hellewell SB, Bruce A, Feinstein G, Orringer J, Williams W, and Bowen WD (1994) Rat liver and kidney contain high densities of sigma 1 and sigma 2 receptors: characterization by ligand binding and photoaffinity labeling. *Eur J Pharmacol* **268**(1): 9-18.

Johannessen M, Ramachandran S, Riemer L, Ramos-Serrano A, Ruoho AE, and Jackson MB (2009) Voltage-gated sodium channel modulation by sigma-receptors in cardiac myocytes and heterologous systems. *Am J Physiol Cell Physiol* **296**(5): C1049-1057.

Kaushal N, Robson MJ, Rosen A, McCurdy CR, and Matsumoto RR (2014) Neuroprotective targets through which 6-acetyl-3-(4-(4-(4-fluorophenyl)piperazin-1-yl)butyl)benzo[*d*]oxazol-2(*3H*)-one (SN79), a sigma receptor ligand, mitigates the effects of methamphetamine in vitro. *Eur J Pharmacol* **724**: 193-203.

Kaushal N, Robson MJ, Vinnakota H, Narayanan S, Avery BA, McCurdy CR, and Matsumoto RR (2011) Synthesis and pharmacological evaluation of 6-acetyl-3-(4-(4-(4-fluorophenyl)piperazin-1-yl)butyl)benzo[d]oxazol-2(3H)-one (SN79), a cocaine antagonist, in rodents. *AAPS J* **13**(3): 336-346.

Kaushal N, Seminerio MJ, Robson MJ, McCurdy CR, and Matsumoto RR (2012) Pharmacological evaluation of SN79, a sigma (sigma) receptor ligand, against methamphetamine-induced neurotoxicity in vivo. *Eur Neuropsychopharmacol.*

Kim A, Im M, Yim NH, and Ma JY (2014) Reduction of metastatic and angiogenic potency of malignant cancer by Eupatorium fortunei via suppression of MMP-9 activity and VEGF production. *Sci Rep* **4**: 6994.

Liang X, Yang D, Hu J, Hao X, Gao J, and Mao Z (2008) Hypoxia inducible factor-alpha expression correlates with vascular endothelial growth factor-C expression and lymphangiogenesis/angiogenesis in oral squamous cell carcinoma. *Anticancer Res* **28**(3A): 1659-1666.

Lin C, McGough R, Aswad B, Block JA, and Terek R (2004) Hypoxia induces HIF-1alpha and VEGF expression in chondrosarcoma cells and chondrocytes. *J Orthop Res* **22**(6): 1175-1181.

Losel RM, Besong D, Peluso JJ, and Wehling M (2008) Progesterone receptor membrane component 1--many tasks for a versatile protein. *Steroids* **73**(9-10): 929-934.

Mach RH, Zeng C, and Hawkins WG (2013) The sigma2 receptor: a novel protein for the imaging and treatment of cancer. *J Med Chem* **56**(18): 7137-7160.

Matsumoto RR, Bowen WD, Tom MA, Vo VN, Truong DD, and De Costa BR (1995) Characterization of two novel sigma receptor ligands: antidystonic effects in rats suggest sigma receptor antagonism. *Eur J Pharmacol* **280**(3): 301-310.

McCurdy CR, Mesangeau C, Matsumoto RR, Poupaert JH, Avery BA, and Abdelazeem AHA (2014) Highly selective sigma receptor ligands. United States of America. **Patent # US8686008 B2**.

Monassier L, Manoury B, Bellocq C, Weissenburger J, Greney H, Zimmermann D, Ehrhardt JD, Jaillon P, Baro I, and Bousquet P (2007) Sigma(2)-receptor ligand-mediated inhibition of inwardly rectifying K(+) channels in the heart. *J Pharmacol Exp Ther* **322**(1): 341-350.

Neubauer H, Adam G, Seeger H, Mueck AO, Solomayer E, Wallwiener D, Cahill MA, and Fehm T (2009) Membrane-initiated effects of progesterone on proliferation and activation of VEGF in breast cancer cells. *Climacteric* **12**(3): 230-239.

Nicholson H, Comeau A, Mesangeau C, McCurdy CR, and Bowen WD (2015) Characterization of CM572, a Selective Irreversible Partial Agonist of the Sigma-2 Receptor with Antitumor Activity. *Journal of Pharmacology and Experimental Therapeutics*.

Ostenfeld MS, Fehrenbacher N, Hoyer-Hansen M, Thomsen C, Farkas T, and Jaattela M (2005) Effective tumor cell death by sigma-2 receptor ligand siramesine involves lysosomal leakage and oxidative stress. *Cancer Res* **65**(19): 8975-8983.

Peluso JJ, Liu X, Gawkowska A, Lodde V, and Wu CA (2010) Progesterone inhibits apoptosis in part by PGRMC1-regulated gene expression. *Mol Cell Endocrinol* **320**(1-2): 153-161.

Shoghi KI, Xu JB, Su Y, He J, Rowland D, Yan Y, Garbow JR, Tu ZD, Jones LA, Higashikubo R, Wheeler KT, Lubet RA, Mach RH, and You M (2013) Quantitative Receptor-Based Imaging of Tumor Proliferation with the Sigma-2 Ligand [F-18]ISO-1. *Plos One* **8**(9).

Talks KL, Turley H, Gatter KC, Maxwell PH, Pugh CW, Ratcliffe PJ, and Harris AL (2000) The expression and distribution of the hypoxia-inducible factors HIF-1alpha and HIF-2alpha in normal human tissues, cancers, and tumor-associated macrophages. *Am J Pathol* **157**(2): 411-421.

Tsai SY, Hayashi T, Mori T, and Su T-P (2009) Sigma-1 receptor chaperones and diseases. *Cent Nerv Syst Agents Med Chem* **9**(3): 184-189.

Vilner BJ and Bowen WD (2000) Modulation of cellular calcium by sigma-2 receptors: release from intracellular stores in human SK-N-SH neuroblastoma cells. *J Pharmacol Exp Ther* **292**(3): 900-911.

Vilner BJ, John CS and Bowen WD (1995) Sigma-1 and sigma-2 receptors are expressed in a wide variety of human and rodent tumor cell lines. *Cancer Res* **55**(2): 408-413.

Wheeler KT, Wang LM, Wallen CA, Childers SR, Cline JM, Keng PC, and Mach RH (2000) Sigma-2 receptors as a biomarker of proliferation in solid tumours. *British Journal of Cancer* **82**(6): 1223-1232.

Xu JB, Zeng CB, Chu WH, Pan FH, Rothfuss JM, Zhang FJ, Tu ZD, Zhou D, Zeng DX, Vangveravong S, Johnston F, Spitzer D, Chang KC, Hotchkiss RS, Hawkins WG, Wheeler KT, and Mach RH (2011) Identification of the PGRMC1 protein complex as the putative sigma-2 receptor binding site. *Nature Communications* **2**.

Zeng C, Rothfuss J, Zhang J, Chu W, Vangveravong S, Tu Z, Pan F, Chang KC, Hotchkiss R, and Mach RH (2012) Sigma-2 ligands induce tumour cell death by multiple signalling pathways. *Br J Cancer* **106**(4): 693-701.

Zeng C, Rothfuss JM, Zhang J, Vangveravong S, Chu W, Li S, Tu Z, Xu J, and Mach RH (2014) Functional assays to define agonists and antagonists of the sigma-2 receptor. *Anal Biochem* **448**: 68-74.

Zhong H, De Marzo AM, Laughner E, Lim M, Hilton DA, Zagzag D, Buechler P, Isaacs WB, Semenza GL, and Simons JW (1999) Overexpression of hypoxia-inducible factor 1alpha in common human cancers and their metastases. *Cancer Res* **59**(22): 5830-5835.

Footnotes:

*This work was supported by the National Institutes of Health National Institute of General Medical Sciences T32 Predoctoral Pharmacology Training Grant [1-T32 GM077995-01A2] (HN); National Institutes of Health National Institute of General Medical Sciences Initiative for Maximizing Student Development Grant [R25 GM083270] (HN); Brown University Pharmacia Pre-doctoral Fellowship in Pharmacology (HN); National Institutes of Health National Institute on Drug Abuse Grant [R01 DA023205] (CM, CRM); National Institutes of Health National Institute of General Medical Sciences Grant [P20 GM104932] (CM, CRM); and the Upjohn Professorship in Pharmacology, Brown University (WDB)

This work has been previously presented in part at the Society for Neuroscience Annual Meeting 2014 (299.17).

JPET Fast Forward. Published on November 16, 2015 as DOI: 10.1124/jpet.115.228387
This article has not been copyedited and formatted. The final version may differ from this version.

Tables

Table 1. **Sigma receptor ligands and their affinities and selectivities**

Common Name	**Chemical Name**	**Sigma-1 Receptor Affinity (nM)**	**Sigma-2 Receptor Affinity (nM)**	**Sigma-2 Receptor Selectivity (fold)**	**References**
SN79	6-acetyl-3-(4-(4-(4-fluorophenyl)piperazin-1-yl)butyl)benzo[d]oxazol-2(3H)-one	27	7	4	Kaushal et al. 2011
CM572	3-(4-(4-(4-fluorophenyl)piperazin-1-yl)butyl)-6-isothiocyanatobenzo[*d*]oxazol-2(3*H*)-one	>10,000	14.6	>685	Nicholson et al. 2015
BD1047	N'-[2-(3,4-dichlorophenyl)ethyl]-N,N,N'-trimethylethane-1,2-diamine	0.93	47	0.02	Matsumoto et al. 1995
NE100	4-methoxy-3-(2-phenylethoxy)-N,N-dipropylbenzeneethanamine	1.54	84.7	0.02	Chaki et al. 1994
BD1063	1-[2-(3,4-dichlorophenyl)ethyl]-4-methylpiperazine	9.15	449	0.02	Matsumoto et al. 1995
(+)-pentazocine	2-dimethylallyl-5,9-dimethyl-2'-hydroxybenzomorphan	7.5	1,542	0.005	Hellewell et al. 1994

JPET Fast Forward. Published on November 16, 2015 as DOI: 10.1124/jpet.115.228387
This article has not been copyedited and formatted. The final version may differ from this version.

Figure legends

Figure 1. **Structures of SN79 and CM764.** CM764 is a novel derivative of the well-characterized sigma-2 antagonist SN79. Addition of an amine to the fluorophenyl ring of SN79 results in CM764. Synthesis of CM764 was described previously (McCurdy et al. 2014). The stability of CM764 was examined using the methods described in supplemental material (Supplemental Figures 1-4). CM764 was found to be stable under the experimental conditions described herein.

Figure 2. **CM764 binding at sigma-1 and sigma-2 receptors.** Affinity of CM764 for sigma-1 and sigma-2 receptors was determined by competition binding in rat liver membranes. Assays were carried out as described in Materials and Methods, using [^{3}H](+)-pentazocine to label sigma-1 receptors and [^{3}H]DTG in presence of unlabeled (+)-pentazocine to label sigma-2 receptors. Results are expressed as the percentage of control specific binding at each concentration of CM764. K_i values were determined by analysis of competition curves using GraphPad Prism 6 and radioligand K_d values previously determined ([^{3}H](+)-pentazocine K_d, 7.5 nM; [^{3}H]DTG K_d, 17.9 nM (Hellewell et al. 1994)). Graphpad analysis revealed Ki values of 86.6 ± 2.8 nM and 3.5 ± 0.9 nM at sigma-1 and sigma-2 receptors, respectively. Each curve represents the average of at least 3 independent experiments ± S.D., with each experiment performed in duplicate.

Figure 3. **Effect of CM764 treatment on MTT reduction in SK-N-SH neuroblastoma.** SK-N-SH neuroblastoma cells were treated with CM764 at the indicated doses for 24 h prior to MTT assay, carried out as described in Materials and Methods. CM764 treatment induced a statistically significant dose-dependent increase in MTT reduction (one-way ANOVA $F=13.94$, Dunnett's post-hoc comparison to control 3 μM $*p<0.05$, 10 μM $***p<0.001$). Results are expressed as an average percent change in MTT reduction ± S.D. in treated samples relative to an untreated control for at least three independent experiments, with each experiment having 5 replicates.

Figure 4. **Effect of CM764 treatment on DNA replication in SK-N-SH neuroblastoma.** DNA replication was measured to determine the effect of CM764 treatment on cellular proliferation using the CyQUANT assay as described in Materials and Methods. There was no significant change in DNA synthesis as measured by CyQUANT GR dye fluorescence in cells treated with CM764 as compared to untreated cells up to 96 h exposure. This indicates that the effect of CM764 on SK-N-SH neuroblastoma does not result in an increase in cellular proliferation. Results are presented as the fold-change in level of nucleotides as measured by ratio of RFU in treated and untreated cells at that time point. Data presented is the average of two independent experiments ± S.D., with each experiment having 5 replicates per condition. Media and ligand were changed after every 24 h period.

Figure 5. **Effect of sigma-2 receptor antagonists on CM764-induced MTT reduction in SK-N-SH neuroblastoma.** Cells were exposed to 10 μM CM764 alone, the indicated antagonist alone, or to the combination of 10 μM CM764 and antagonist for 24 h. MTT reduction was measured as described in Materials and Methods. No antagonist alone produced a significant effect on MTT reduction as compared to an untreated control. All antagonists were able to significantly attenuate the stimulative effect of CM764 on MTT reduction (one-way ANOVA $F=13.73$). CM572 and SN79, the most highly sigma-2 selective antagonists investigated, were both able to fully attenuate CM764-induced increase in MTT reduction (Dunnett's test for multiple comparisons as compared to an untreated control, ****$p<0.0001$). The other sigma-2 antagonists, though more selective for sigma-1 receptors, were also able to significantly attenuate CM764-induced MTT reduction (BD1047 ***$p<0.001$; NE100 **$p<0.01$; BD1063 **$p<0.01$). The data support the notion that the effect is sigma-2 receptor-mediated. Results are presented as an average increase in MTT reduction as compared to an untreated control for at least 3 independent experiments, with each experiment performed with 5 replicates.

Figure 6. **Effect of CM764 treatment on intracellular calcium in SK-N-SH neuroblastoma.** Cells were loaded with fura-2,AM for 60 min. prior to CM764 or vehicle injection (injection indicated by black arrow). CM764 injection induced an immediate increase in cytosolic calcium in SK-N-SH neuroblastoma, as has been previously demonstrated in response to sigma-2 receptor activation. A representative trace for each condition is shown. Data is presented as a change in intracellular calcium level with the baseline removed, with the baseline level of calcium determined by the average of 25 ratio measurements prior to injection. Experiment was repeated 4 times with similar results, with each experiment having 4 replicates.

Figure 7. **Changes in NADH/NAD$^+$ in response to CM764 exposure.** Cells were exposed to 10 μM CM764 for 24 h prior to NADH/NAD$^+$ assay, carried out as described in Methods. Treatment with CM764 induced a statistically significant, yet not robust ~1.4-fold increase in total NAD (NADH + NAD$^+$) as compared to an untreated control (Student's t-test, $p<0.05$ ($p=0.043$)). NADH and NAD$^+$ levels each showed a similar trend to total NAD, but did not reach statistical significance. Results are presented as an average fold increase in absorbance in treated wells as compared to an untreated control for 3 independent experiments ± S.D., with each experiment being performed in triplicate.

Figure 8. **Changes in ATP levels in response to CM764 exposure.** Cells were exposed to 10 μM CM764 for 24 h prior to ATP assay as described in Methods. Treatment with CM764 induced a ~13% increase in ATP level as compared to an untreated control (Student's t-test, *$p<0.05$ ($p=0.032$)). Results are presented as an average % change in ATP levels as determined by an increase in relative fluorescence normalized to protein concentration in treated cells compared to an untreated control for 3 independent experiments and controlled for cell number in 1 experiment for a total of 4 independent experiments ± S.D., with each experiment being performed in duplicate.

Figure 9. **Effect of CM764 on reactive oxygen species levels in SK-N-SH neuroblastoma cells.** Cells were stained with DCFDA prior to treatment with 10 μM CM764 for 4 h, followed by fluorescence measurement as described in Methods. Panel A demonstrates the effectiveness

of the assay, showing the effect of 500 μM tert-butyl hydrogen peroxide (TBHP) as a positive control for the production of reactive oxygen species. Panel B shows the results of treatment with the antioxidant α-tocopherol (Vitamin E, 200 μg/ml) and treatment with 10 μM CM764. Treatment of SK-N-SH neuroblastoma cells with CM764 resulted in a marked decrease in reactive oxygen species that was more effective than that of α-tocopherol (95% and 76%, respectively). Results were highly significant (one-way ANOVAF=238.4, Dunnett's test for multiple comparisons as compared to the untreated control ****$p<0.0001$ for α-tocopherol, ****$p<0.0001$ for CM764). Results are presented as an average of the percent change in ROS levels achieved ± S.D. as compared to an untreated control normalized to 100% for three independent experiments, each experiment having four replicates per condition.

Figure 10. **Effect of CM764 treatment on levels of HIF1α in SK-N-SH neuroblastoma.** Cell lysates of SK-N-SH neuroblastoma cells were made after treatment with 10 μM CM764 for the indicated amount of time and were used for Western blotting for HIF1α as described in Materials and Methods. Panel A: HIF1α Western blot and GAPDH loading control. Panel B: Independent blots were quantified and ratio of HIF1α/GAPDH determined and averaged for all experiments. Data is expressed as fold increase in ratio relative to control treated without CM764. Treatment with CM764 resulted in an increase in HIF1α level as early as 3 h after exposure (one-way ANOVA F=8.716, Dunnett's test for multiple comparisons as compared to untreated control *$p<0.05$). Results are an average of two independent experiments. A representative blot is shown.

Figure 11. **Effect of CM764 treatment on expression of VEGF in SK-N-SH neuroblastoma.** Cell lysates of SK-N-SH neuroblastoma cells were made after treatment with 10 μM CM764 for indicated amount of time and were used for Western blotting for VEGF as described in Materials and Methods. Panel A: VEGF Western blot and β-tubulin loading control. Panel B: Independent blots were quantified and ratio of VEGF/loading control (β-tubulin or GAPDH) determined and averaged for all experiments. Data is expressed as fold increase in ratio relative to control treated without CM764. Treatment with CM764 induced protein expression of VEGF after 24 h exposure, following an earlier increase in HIF1α expression as shown in Figure 10 (one-way ANOVA $F=6.558$, Dunnett's test for multiple comparisons as compared to untreated control $^{**}p<0.01$). Results shown are an average of three independent experiments. A representative blot is shown.

Figure 12. **Effect of CM764 treatment across cell types of different tissues.** Human SK-N-SH neuroblastoma, HEK293T human embryonic kidney cells, and MG-63 human osteosarcoma cells were treated with the indicated dose of CM764 for 24 h. MTT assay was then carried out as described in Materials and Methods. CM764 treatment induced an increase in reduction of MTT reagent in all three cell types examined. These data indicate that the effect of CM764 observed in the neuroblastoma is not a cell line-specific effect but is consistent across multiple cell types, both cancerous and non-cancerous. Results are shown as an average percent change in MTT reduction ± S.D. as compared to an untreated control in each cell line for at least three independent experiments, with each experiment performed with 5 replicates.

JPET Fast Forward. Published on November 16, 2015 as DOI: 10.1124/jpet.115.228387
This article has not been copyedited and formatted. The final version may differ from this version.

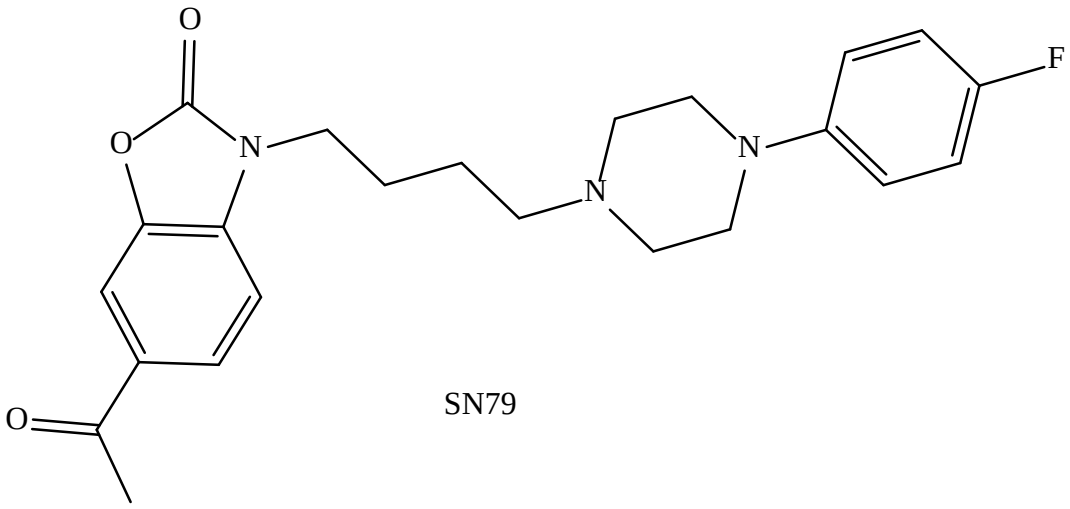

SN79

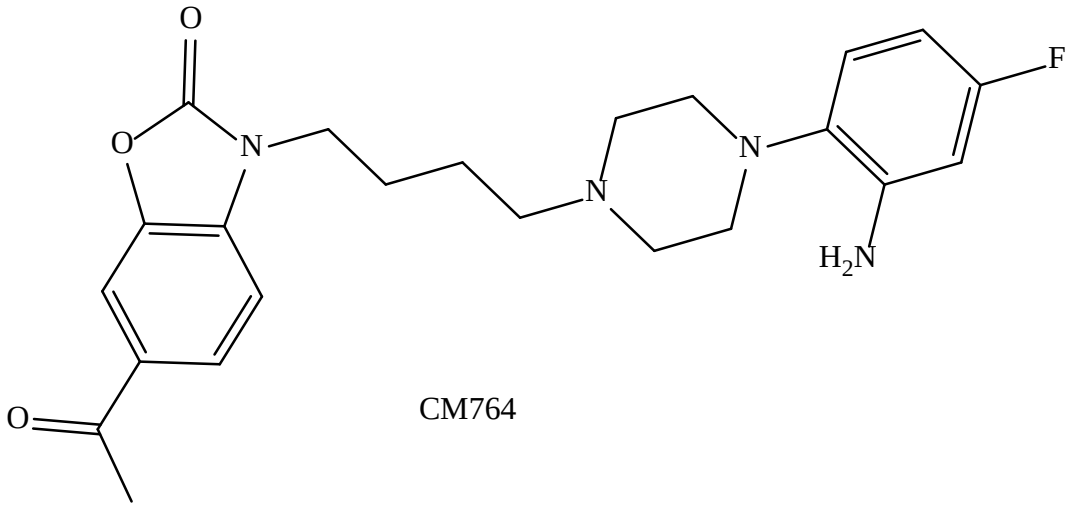

CM764

Figure 1

JPET Fast Forward. Published on November 16, 2015 as DOI: 10.1124/jpet.115.228387
This article has not been copyedited and formatted. The final version may differ from this version.

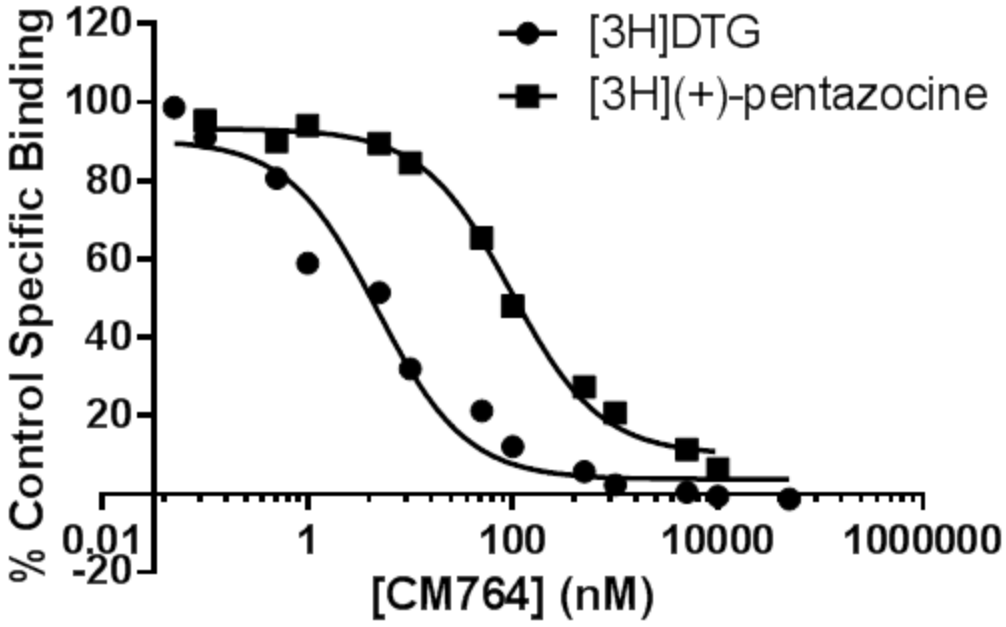

Figure 2

JPET Fast Forward. Published on November 16, 2015 as DOI: 10.1124/jpet.115.228387
This article has not been copyedited and formatted. The final version may differ from this version.

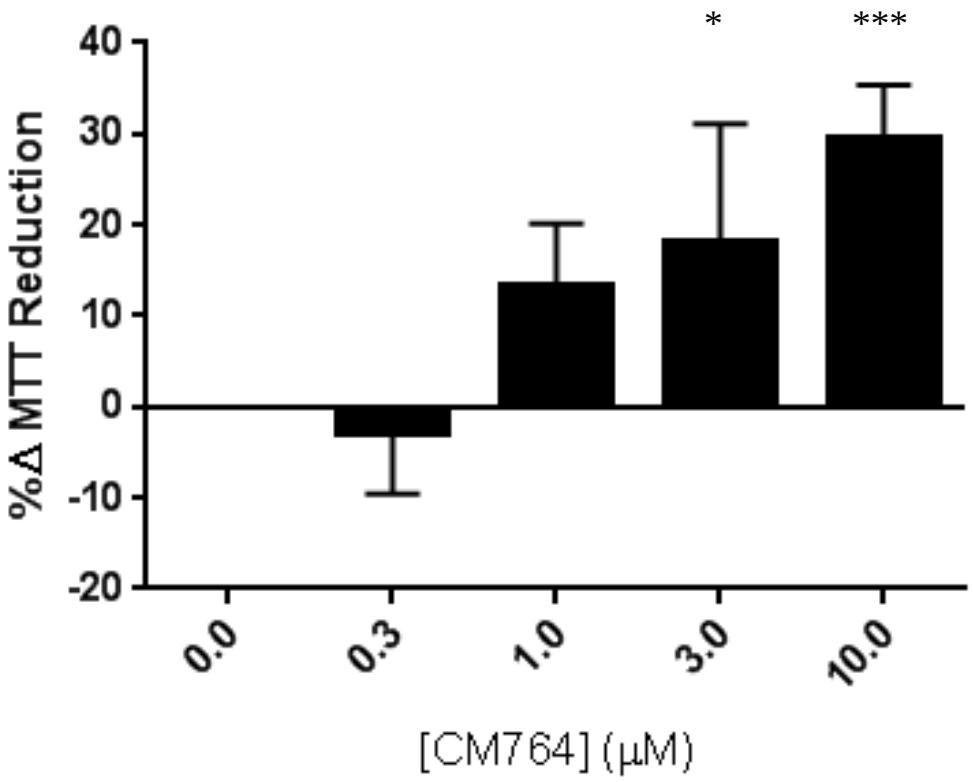

Figure 3

JPET Fast Forward. Published on November 16, 2015 as DOI: 10.1124/jpet.115.228387
This article has not been copyedited and formatted. The final version may differ from this version.

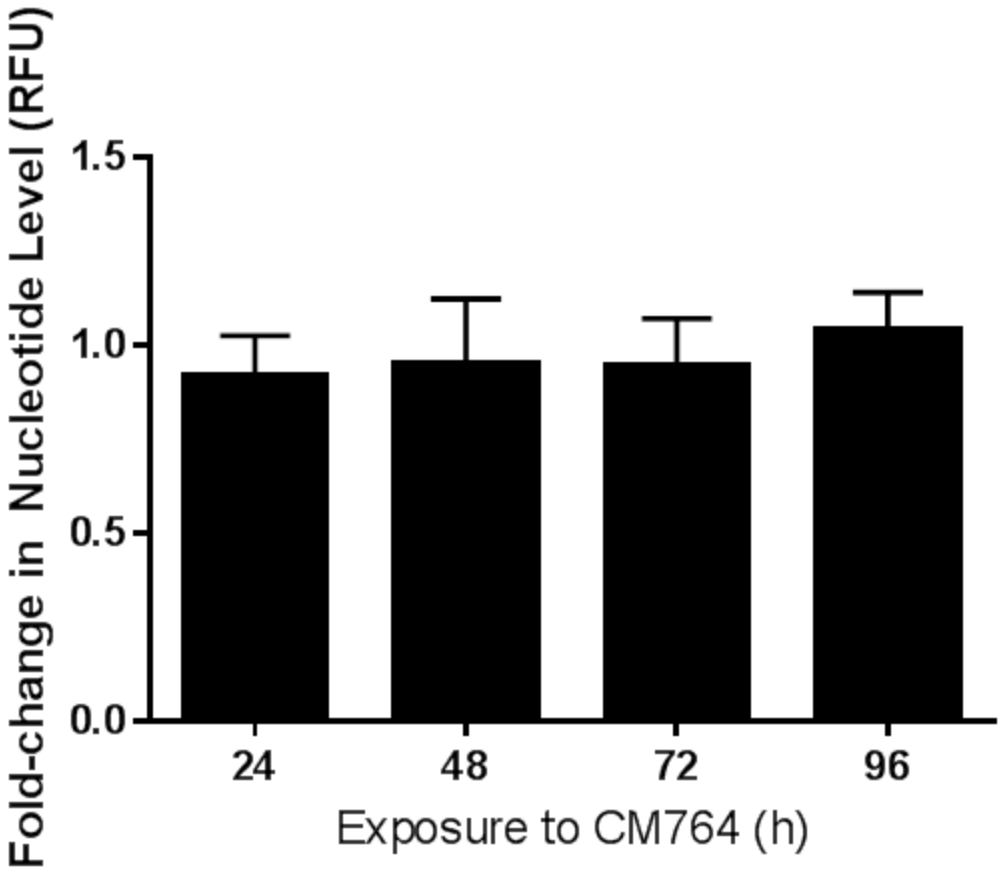

Figure 4

JPET Fast Forward. Published on November 16, 2015 as DOI: 10.1124/jpet.115.228387
This article has not been copyedited and formatted. The final version may differ from this version.

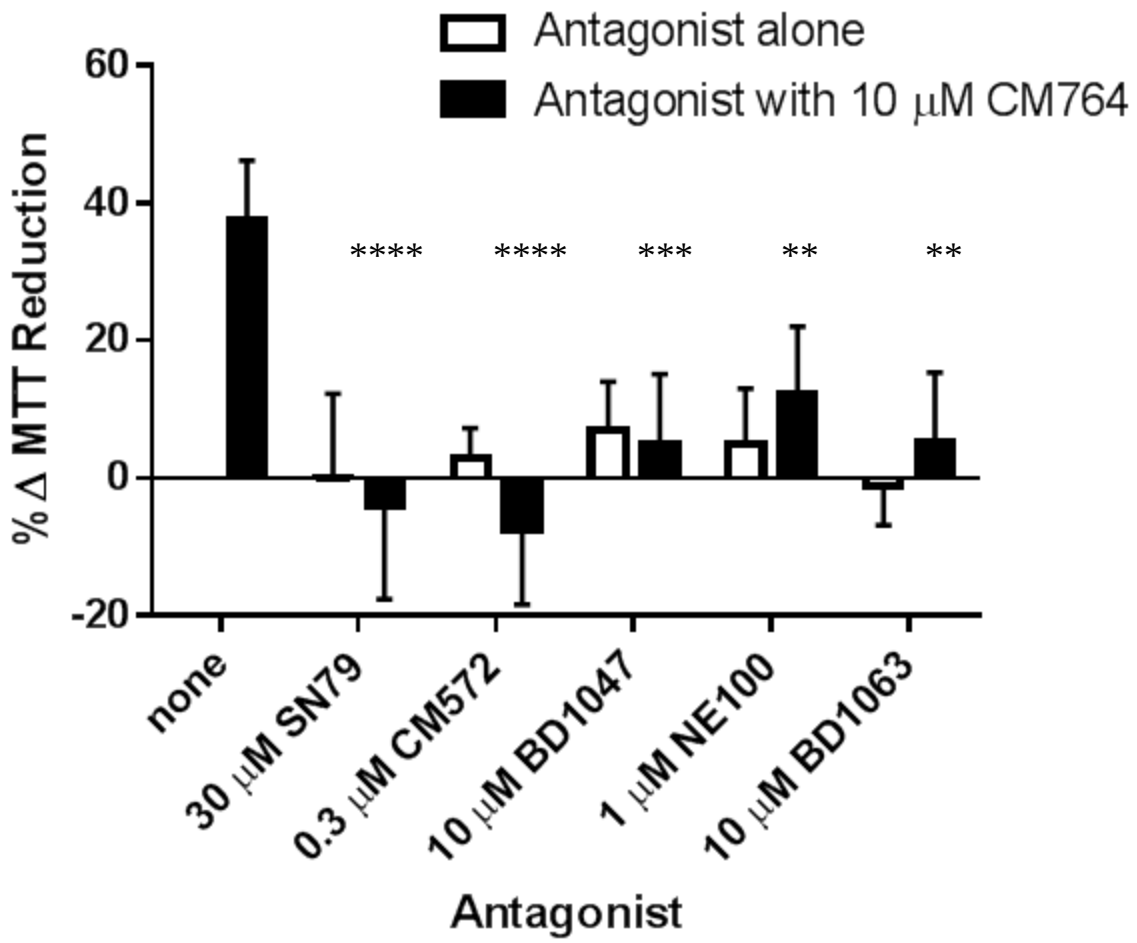

Figure 5

JPET Fast Forward. Published on November 16, 2015 as DOI: 10.1124/jpet.115.228387
This article has not been copyedited and formatted. The final version may differ from this version.

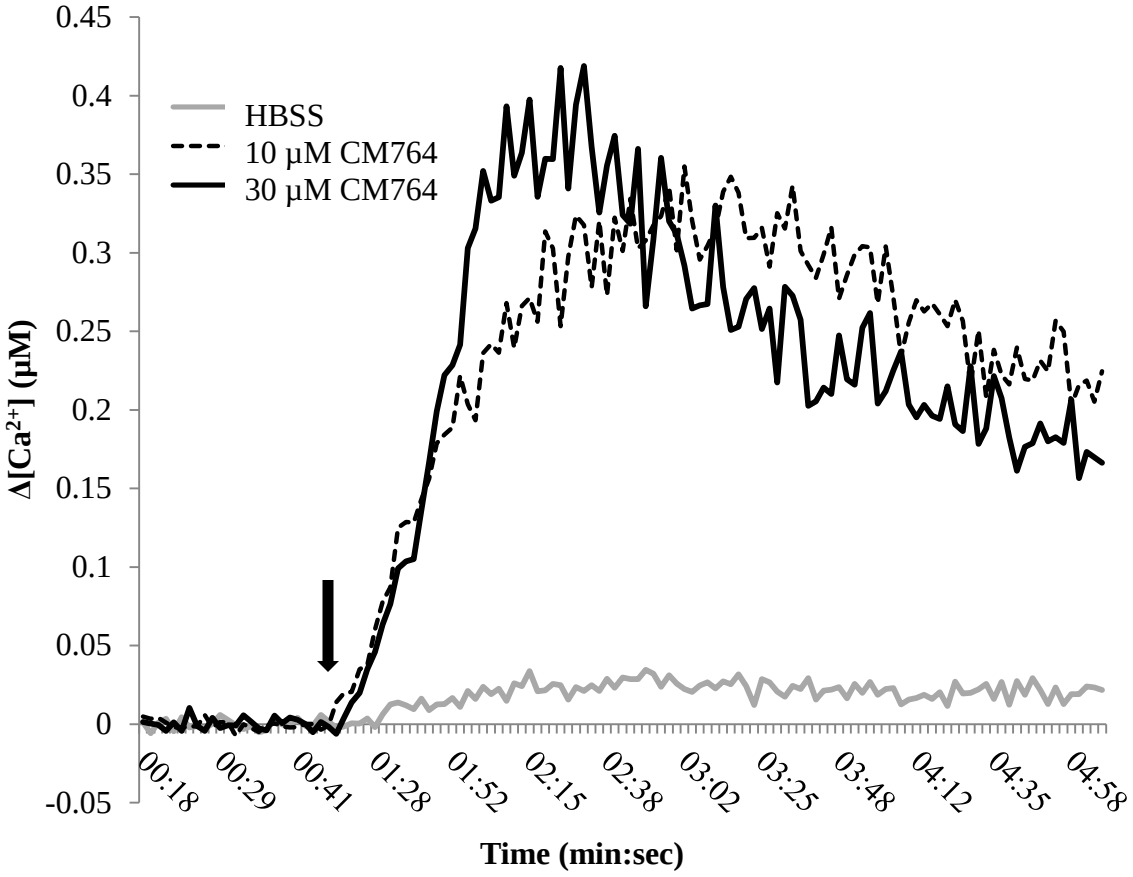

Figure 6

JPET Fast Forward. Published on November 16, 2015 as DOI: 10.1124/jpet.115.228387
This article has not been copyedited and formatted. The final version may differ from this version.

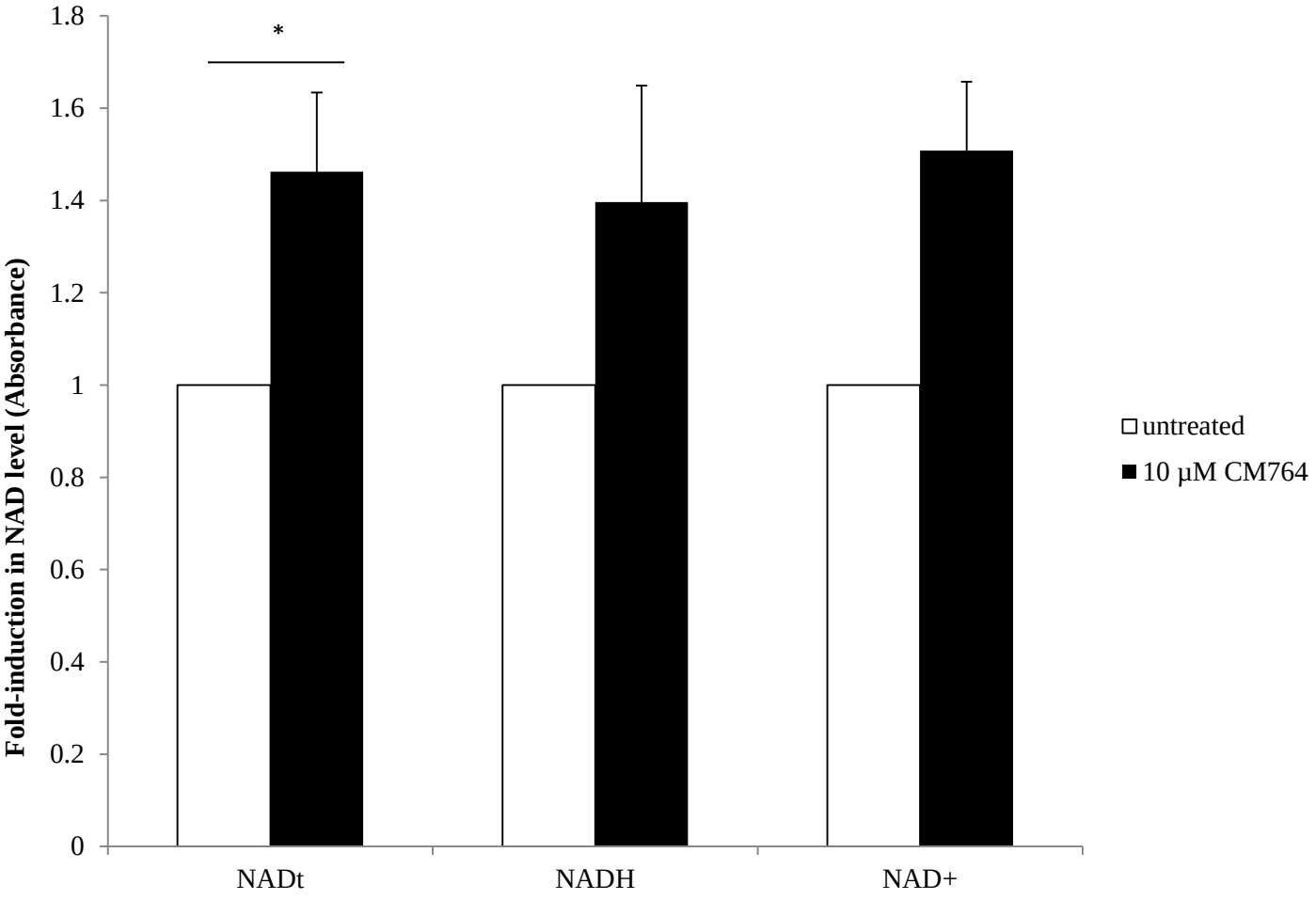

Figure 7

JPET Fast Forward. Published on November 16, 2015 as DOI: 10.1124/jpet.115.228387
This article has not been copyedited and formatted. The final version may differ from this version.

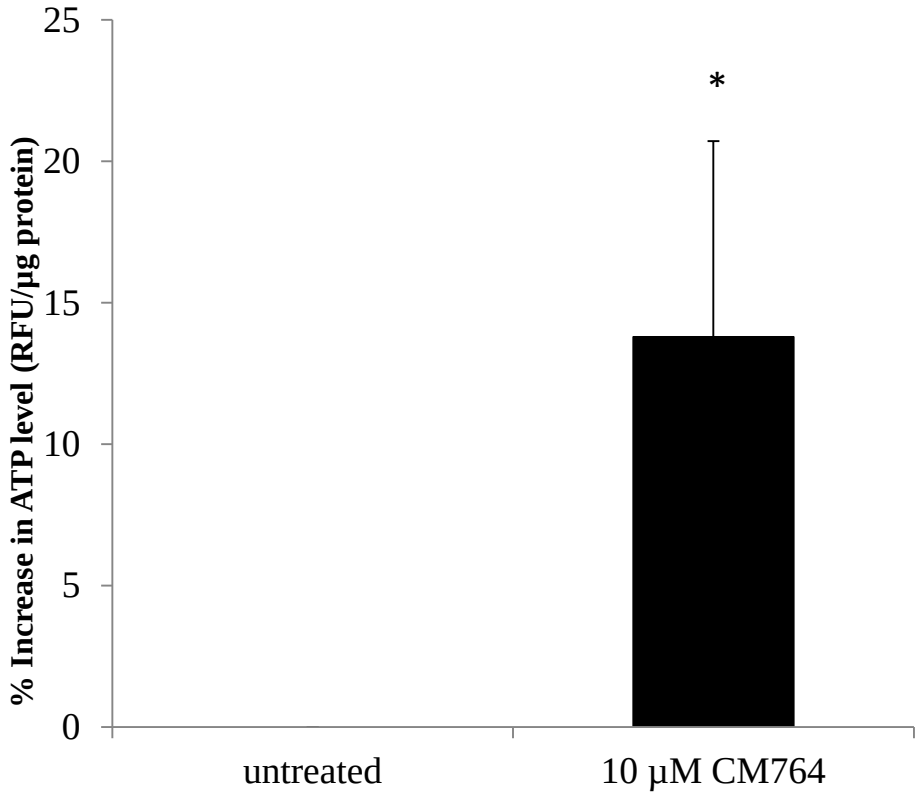

Figure 8

JPET Fast Forward. Published on November 16, 2015 as DOI: 10.1124/jpet.115.228387
This article has not been copyedited and formatted. The final version may differ from this version.

A

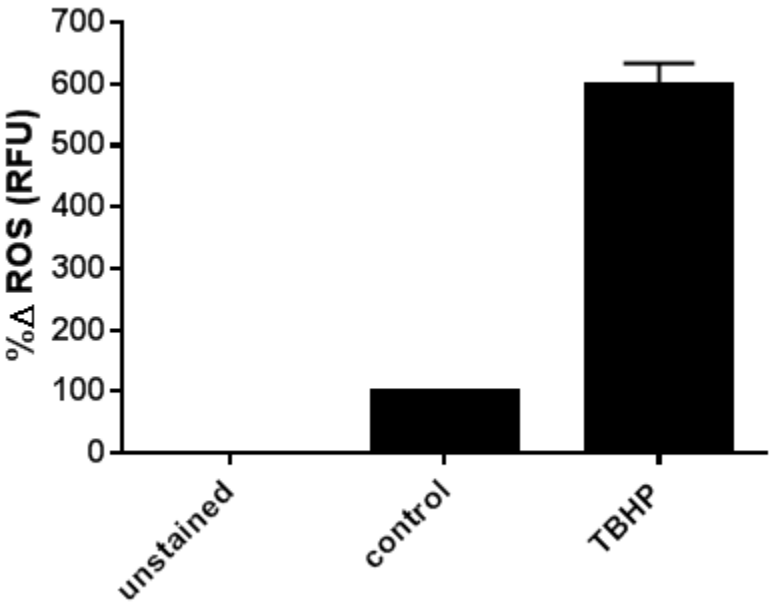

B

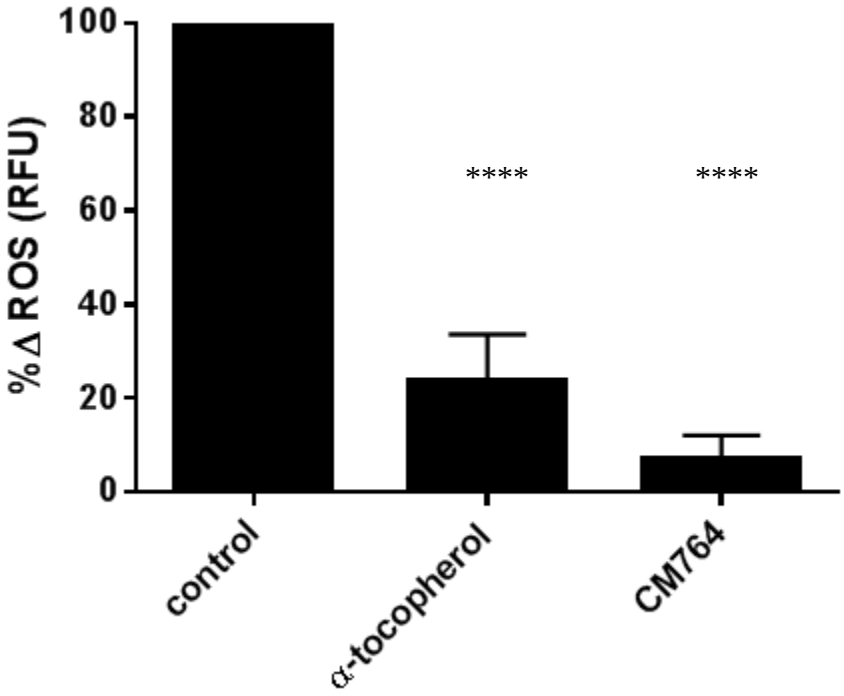

Figure 9

JPET Fast Forward. Published on November 16, 2015 as DOI: 10.1124/jpet.115.228387
This article has not been copyedited and formatted. The final version may differ from this version.

JPET Fast Forward. Published on November 16, 2015 as DOI: 10.1124/jpet.115.228387
This article has not been copyedited and formatted. The final version may differ from this version.

A

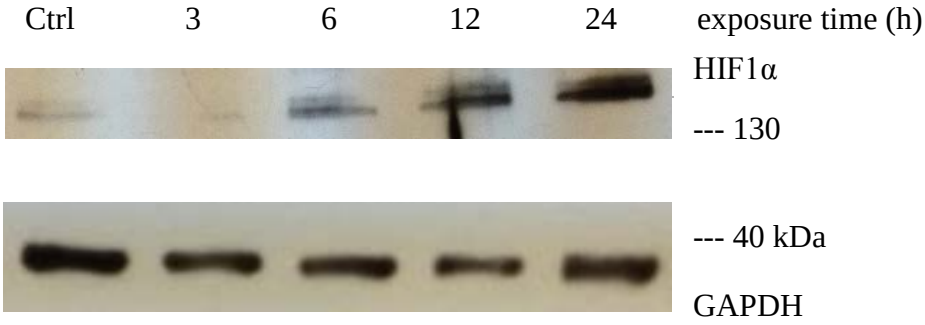

B

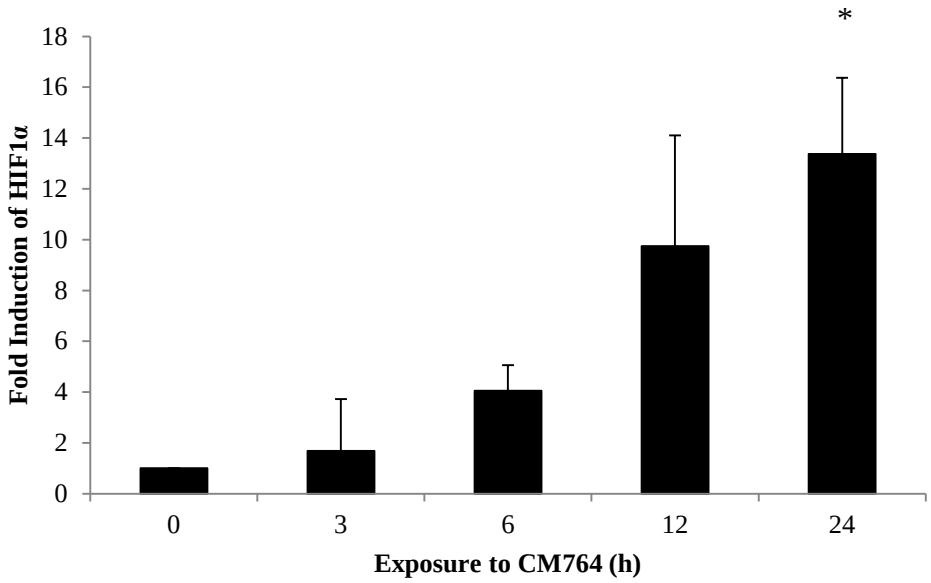

Figure 10

JPET Fast Forward. Published on November 16, 2015 as DOI: 10.1124/jpet.115.228387
This article has not been copyedited and formatted. The final version may differ from this version.

A

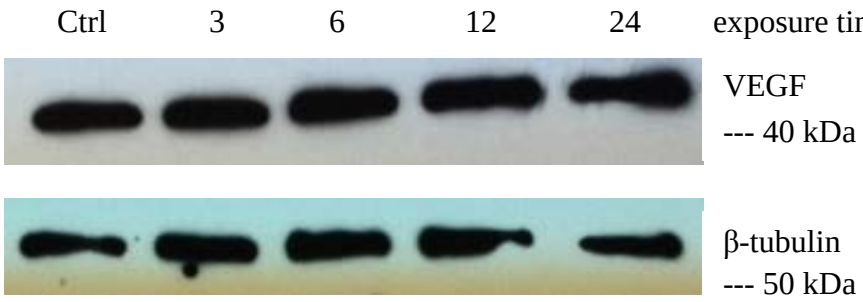

B

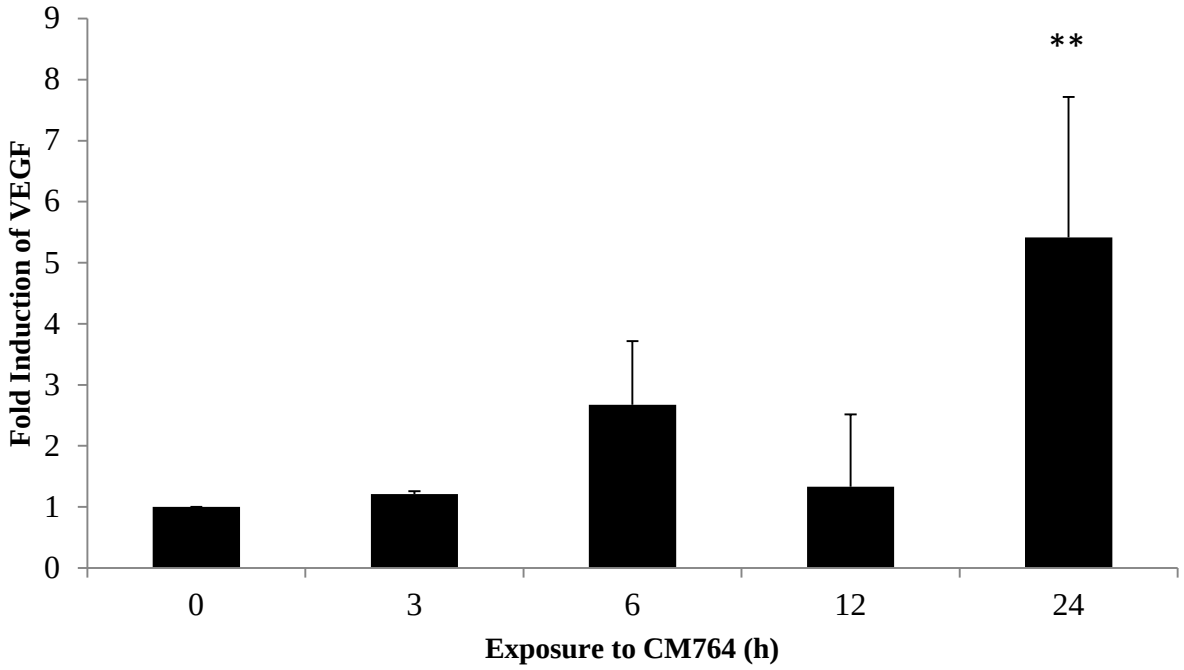

Figure 11

JPET Fast Forward. Published on November 16, 2015 as DOI: 10.1124/jpet.115.228387
This article has not been copyedited and formatted. The final version may differ from this version.

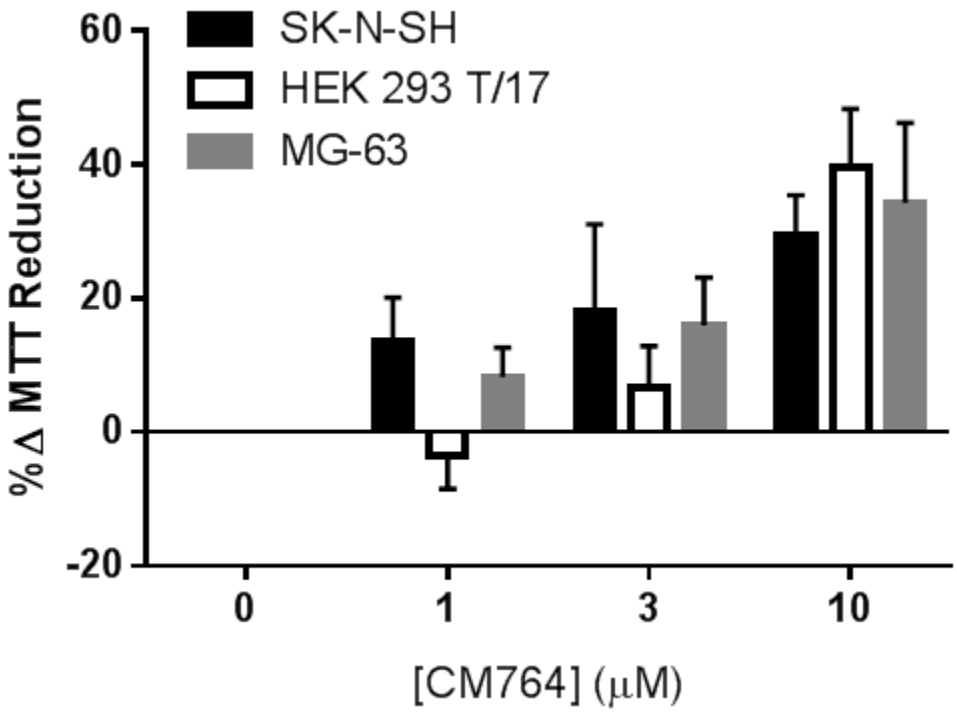

Figure 12